ISSN 2347-1921

PARAMETERS EFFECTS ON CONDUCTION-CONVECTION HEAT TRANSFER IN RECTANGULAR ENCLOSURE SANDWICHED BY FINITE THICKNESS WALLS

Ahmed M. Jumaa, Ameer S. Dawood, Hekmat Sh. Mustafa
Department of Mathematics, College of Computer Sciences & Mathematics, University of Mosul, Iraq
altaieahm@yahoo.com
Department of Mechanical Engineering, College of Engineering, University of Mosul, Iraq
amirsd1954@yahoo.com
Department of Mathematics, College of Computer Sciences & Mathematics, University of Mosul, Iraq
heksha@yahoo.com

ABSTRACT

The effect of wall heat conduction on natural convection heat transfer in cavities has gained attention of many researchers in recent years due to its wide application areas in engineering such that building heating and cooling and thick enclosures, etc.

In this work, we consider a two-dimensional numerical study of a rectangle cavity filled with an air with two vertical conductive walls of finite thickness. The enclosure is subjected to horizontal temperature gradient, the vertical boundaries are isothermal at different temperatures whereas the remaining walls are adiabatic. The theoretical study involved the numerical solution of the Navier-stokes and energy equations by using finite difference method. The stream-vorticity formulation was used in the mathematical model. The physical problem depends on five parameters: Rayleigh number $(1000<Ra<1000000)$, the Prandtl number $(Pr=0.7)$, the wall to fluid thermal conductivity ratio $(0.1\leq Kr\leq 10)$, solid to fluid thickness ratio $(0.5\leq L1/L2\leq 1.5)$, the ratio of (left or right) solid thickness to the height $(D=\frac{L1}{H}=0.5,0.6667,0.75)$ and the aspect ratio $(H/L=0.5,1,1.5)$. The main focus of the study is on examining the effect of conduction in the wall on the natural convection flow. The results are presented to show the effect of these parameters on the heat transfer and fluid flow characteristics.

Keywords

conduction-convection heat transfer; finite thickness walls; rectangular enclosure; finite difference method; the ratio of (left or right) solid thickness to the height.

Council for Innovative Research
Peer Review Research Publishing System
Journal: JOURNAL OF ADVANCES IN MATHEMATICS
Vol .10, No 1
www.cirjam.com , editorjam@gmail.com

ISSN 2347-1921

1.INTRODUCTION

The effect of wall heat conduction on natural convection heat transfer in cavities has gained attention of many researchers in recent years due to its wide application areas in engineering such as building heating and cooling, thick walled enclosures, cooling of electronic equipments, internal combustion engines and solar collectors. Moreover, researchers have performed several numerical and experimental studies on natural convection to investigate the effect of wall heat conduction on heat transfer.

The problem of natural convection flow in a square and rectangular enclosure with uniform temperature at vertical walls and insulated top and bottom walls has been the subject of many studies for example: Jones (1979). Effect of wall conductance on natural convection in differently oriented square cavities was studied by Kim and Viskanta (1984). Baytas et al. (2001) studied steady-state conjugate natural convection in a square cavity filled with a porous media. Yedder and Bilgen (1997) analyzed laminar natural convection in an inclined enclosure bounded by a solid wall with its outer boundary at constant temperature while the opposing side has a constant heat flux. Kimura, Tiwata, Okajima and Pop (1997) presented a review of conduction-convection conjugated natural convection from plates or bodies in a fluid-saturated porous medium. The coupled heat transfers in vertical alveolar building envelopes formed by hollow clay tiles have been studied by Abdelbaki and Zrikem (1999). Kikuchi *et al*. (2004) numerically investigated the 2-D conduction effect of vertical walls on natural convection of sodium in a square enclosure and showed that non-uniform temperature distribution at fluid-wall interface caused an enhancement in heat transfer for low conducting stainless steel wall.

Steady conjugate natural-conduction heat transfer in a two-dimensional porous enclosure with finite wall thickness was studied numerically by Saeid (2007). Varol et al. (2008) studied a porous enclosure bounded by two solid massive walls from vertical sides at different thicknesses. Natural convection inside a two-dimensional cavity with a wavy right vertical wall has been studied by Dalal and Das (2008).Aminossadati and Ghasemi (2009) numerically studied natural convection in a partially heated enclosure from below and filled with different types of nanofluids and found that at low Rayleigh numbers a 20% addition of these nanoparticles to pure water resulted in a 42.8% reduction of the heat source maximum temperature. In the study of Basac et al. (2009), heat flow patterns in the presence of natural convection within trapezoidal enclosures have been analyzed with heatlines concept.

The aim of the present study is to investigate the effect of wall heat conduction on natural convection heat transfer in a rectangular cavity filled with an air with two vertical conductive walls of finite thickness.

The governing equations for the problem which are continuity, momentum and energy equations are presented . The continuity and the momentum equations are transformed to the stream function and the vorticity equations . The boundary conditions for all dependent variables are also described. The set of governing equations are solved by finite difference method with the selected finite difference solution technique .

The results will be illustrated for Rayleigh number$(10^3 \leq \mathrm{Ra} \leq 10^6)$,Prandtl number(Pr=0.7), thermal conductivity ratio $(0.1 \leq \mathrm{kr} \leq 10)$, solid to fluid thickness ratio$(\mathrm{L}_1/\mathrm{L}_2 = 0.5,1,1.5)$,the ratio of (left or right) solid thickness to the height $(\mathrm{D} = \frac{\mathrm{L1}}{\mathrm{H}} = 0.5,0.6667,0.75)$ and the aspect ratio (H/L= 0.5,1,1.5).

2. PROBLEM FORMULATION AND GOVERNING EQUATIONS

The physical problem is modelled as a two-dimensional rectangular enclosure with a horizontal length L and a height H. The left and right vertical walls have a thickness L_1. The vertical walls of the enclosure are maintained at different T_h (left wall) and T_c (right wall) constant temperature such that T_h is greater than $\mathrm{T}_\mathrm{c}(\mathrm{T}_\mathrm{h} > \mathrm{T}_\mathrm{c})$, while the horizontal walls are insulated. The fluid part between two vertical walls is considered for air with Prandtl number (Pr=0.7) and for Rayleigh number changing from (10^3) to (10^6).

The following assumptions are made for the problem:

(i) The flow is laminar and two-dimension.

(ii) The fluid is Newtonian viscous, and incompressible.

(iii) Fluid properties are constants except in the buoyancy term consideration.

(iv) Viscous dissipation term is negligible.

ISSN 2347-1921

(v) Heat flow by radiation is negligible.

(vi) No internal heat source or heat sink is involved.

(vii) The boussinesq approximation is invoked for the fluid properties to relate density changes to temperature changes.

NOMENCLATURE

x x-coordinate, (m) . g gravitational acceleration, $(m.s^{-2})$.
X non-dimensional X-coordinate . L length of the cavity , (m) .
Y y-coordinates, (m). L_1 thickness of the solid walls,(m). Y non-dimensional Y-coordinate. $\left(\frac{L_1}{L}\right)$non-dimensional wall thickness.
u velocity component in x-direction,$(m.s^{-1})$. T time, (s).
U non-dimensional velocity component in X-direction.Greek symbols
v velocity component in y-direction, $(m.s^{-1})$. Ψ dimensionless stream function.
V non-dimensional velocity component in Y-direction. Ω dimensionless vorticity.
Ra Rayleigh number, $(g\beta(T_h - T_c)L^3/\vartheta\alpha).\theta$ non-dimensional temperature .
Pr Prandtl number, (ϑ/α) . α effective thermal diffusivity, $(m^2.s^{-1})$.
P non-dimensional pressure. β coefficient of thermal expansion, (K^{-1}).
T dimensional temperature,(K). ϑ kinematic viscosity $(m^2.s^{-1})$.
k_f thermal conductivity of the fluid, $(W.m^{-1}.k^{-1}).\rho$ density, $(kg.m^3)$.
$k_s$thermal conductivity of the wall,$(W.m^{-1}.k^{-1})$.τ non-dimensional time.
kr thermal conductivity ratio,(k_s/k_f). Subscripts
D the ratio of (left or right) solid thickness to the height(D=$\frac{L1}{H}$). c cold.
H height of the cavity, (m) . h hot.
F_y body force, (N) . f fluid part.
Nu local Nusselt number. s solid part.
$\overline{Nu}$ average Nusselt number.

The governing equations for the problem can be written as follow:

Fluid Part

Continuity Equation

$$\frac{\partial u}{\partial x}+\frac{\partial v}{\partial y}=0 \quad \ldots\ldots\ldots\ldots\ldots\ldots(1)$$

Momentum Equation (x-direction)

$$\frac{\partial u}{\partial t}+u\frac{\partial u}{\partial x}+v\frac{\partial u}{\partial y}=-\frac{1}{\rho}\frac{\partial p}{\partial x}+\vartheta\left(\frac{\partial^2 u}{\partial x^2}+\frac{\partial^2 u}{\partial y^2}\right) \quad \ldots\ldots\ldots\ldots\ldots\ldots(2)$$

Momentum Equation (y-direction)

$$\frac{\partial v}{\partial t}+u\frac{\partial v}{\partial x}+v\frac{\partial v}{\partial y}=-\frac{1}{\rho}\frac{\partial p}{\partial y}+\vartheta\left(\frac{\partial^2 v}{\partial x^2}+\frac{\partial^2 v}{\partial y^2}\right)+F_y \quad \ldots\ldots\ldots\ldots\ldots\ldots(3)$$

Energy Equation

$$\frac{\partial T_f}{\partial t}+u\frac{\partial T_f}{\partial x}+v\frac{\partial T_f}{\partial y}=\alpha\left(\frac{\partial^2 T_f}{\partial x^2}+\frac{\partial^2 T_f}{\partial y^2}\right) \quad \ldots\ldots\ldots\ldots\ldots\ldots(4)$$

ISSN 2347-1921

Solid Part

Energy Equation

$$\frac{\partial T_s}{\partial t} = \alpha\left(\frac{\partial^2 T_s}{\partial x^2}+\frac{\partial^2 T_s}{\partial y^2}\right) \quad \text{.....(5)}$$

The body force per unit mass due to buoyancy in the y-direction (F_y) can be obtained by the boussinesq approximation:

$$\rho = \rho_0\left(1+\beta(T-T_c)\right) \text{.....(6)}$$

Where (β) is the volume coefficient of thermal expansion and (ρ_0) is the bulk fluid density .Thus, the body force (F_y) becomes:

$$F_y = g\beta(T-T_c) \quad \text{.....(7)}$$

Then, the y-momentum equation (3) becomes:

$$\frac{\partial v}{\partial t}+u\frac{\partial v}{\partial x}+v\frac{\partial v}{\partial y}=-\frac{1}{\rho}\frac{\partial p}{\partial y}+\vartheta\left(\frac{\partial^2 v}{\partial x^2}+\frac{\partial^2 v}{\partial y^2}\right)+g\beta\,(T-T_c) \quad \text{.....(8)}$$

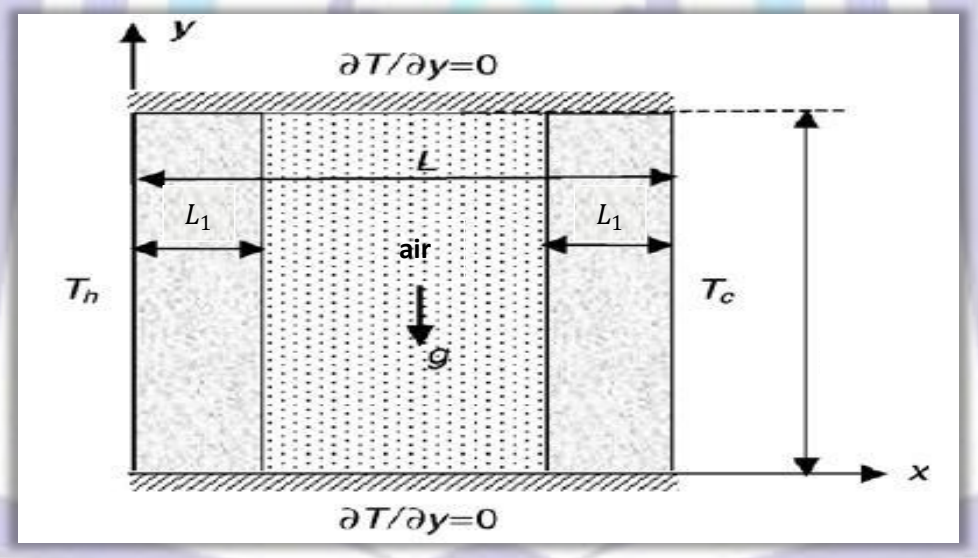

Fig.1:Schematic diagram of the physical model and coordinate system

2.1 Initial And Boundary Conditions

The governing equations are subjected to the following initial and boundary conditions:

Initial Conditions

$$T = T_c \;,\; u = v = 0 \quad at \quad t = 0 \quad \text{.....(9)}$$

Boundary Conditions $for\ t > 0$:

$$T = T_h \;,\; u = v = 0 \quad at \quad x = 0 \;,\; 0 < y < H \text{.....(10a)}$$

ISSN 2347-1921

$T = T_c \quad , \quad u = v = 0 \quad atx = L \quad , \quad 0 < y < H$.....(10b) $\frac{\partial T}{\partial y} = 0 \quad , \quad u = v = 0 \quad aty = 0 \quad , \quad 0 < x < L$.....(10c) $\frac{\partial T}{\partial y} = 0 \quad , \quad u = v = 0 \quad aty = H \quad , \quad 0 < x < L$ .....(10d) $T_f = T_s \, , K_f \frac{\partial T_f}{\partial x} = K_s \frac{\partial T_s}{\partial x} atx = L_1 and x = L_1 + L_2 \, , \; 0 < y < L$ .....(10e)

2.2 Dimensionless Form Of The Governing Equations

The governing equations are made dimensionless using the following non-dimensionalizing parameters:

$$X = \frac{x}{L} \, , \quad Y = \frac{y}{L} \, , U = \frac{uL}{\alpha} \, , V = \frac{vL}{\alpha} \, , \tau = \frac{t\alpha}{L^2} \, , \theta = \frac{T - T_c}{T_h - T_c} \, , P = \frac{pL^2}{\rho \alpha^2}$$

The governing equations (1)-(8) reduce to non-dimensional form:

$$\frac{\partial U}{\partial X} + \frac{\partial V}{\partial Y} = 0 \qquad \text{.....(11)}$$

$$\frac{\partial U}{\partial \tau} + U\frac{\partial U}{\partial X} + V\frac{\partial U}{\partial Y} = -\frac{\partial P}{\partial X} + Pr\left(\frac{\partial^2 U}{\partial X^2} + \frac{\partial^2 U}{\partial Y^2}\right) \qquad \text{.....(12)}$$

$$\frac{\partial V}{\partial \tau} + U\frac{\partial V}{\partial X} + V\frac{\partial V}{\partial Y} = -\frac{\partial P}{\partial Y} + Pr\left(\frac{\partial^2 V}{\partial X^2} + \frac{\partial^2 V}{\partial Y^2}\right) + RaPr\theta \qquad \text{.....(13)}$$

$$\frac{\partial \theta_f}{\partial \tau} + U\frac{\partial \theta_f}{\partial X} + V\frac{\partial \theta_f}{\partial Y} = \frac{\partial^2 \theta_f}{\partial X^2} + \frac{\partial^2 \theta_f}{\partial Y^2} \qquad \text{.....(14)}$$

$$\frac{\partial \theta_s}{\partial \tau} = \alpha^* \left[\frac{\partial^2 \theta_s}{\partial X^2} + \frac{\partial^2 \theta_s}{\partial Y^2}\right] \qquad \text{.....(15)}$$

Where: $Pr = \frac{\vartheta}{\alpha} = \frac{\mu C_p}{K}$ is a prandtl number, $\mathrm{Ra} = \frac{\mathrm{g}\,\beta\,(\mathrm{T_h} - \mathrm{T_c})\mathrm{L}^3}{\vartheta\alpha}$ is a Rayleigh number and $\alpha^* = \frac{\alpha_s}{\alpha_f}$ is the diffusivity ratio, we take $\alpha^* = 1$.

Normalized X and Y moment equations are combined together to eliminate the pressure terms, we shall define a dimensionless stream function Ψ and vorticity Ω as follow:

$$U = \frac{\partial \Psi}{\partial Y} \quad , \quad V = -\frac{\partial \Omega}{\partial X} \qquad \text{.....(16)}$$

and

$$\Omega = \frac{\partial V}{\partial X} - \frac{\partial U}{\partial Y} \qquad \text{.....(17)}$$

Eliminating the pressure terms in equations (12) and (13) by cross differentiation (differentiate equation (12) with respect to Y and equation (13) with respect to X). We can express the resulting equations in terms of dimensionless stream function, vorticity and the energy as:

$$\frac{\partial^2 \Psi}{\partial X^2} + \frac{\partial^2 \Psi}{\partial Y^2} = -\Omega \qquad \text{.....(18)}$$

ISSN 2347-1921

$$\frac{\partial \theta_s}{\partial \tau} = \frac{\partial^2 \theta_s}{\partial X^2} + \frac{\partial^2 \theta_s}{\partial Y^2} \quad \text{.....(19)}$$

$$\frac{\partial \Omega}{\partial \tau} + \frac{\partial \Psi}{\partial Y}\frac{\partial \Omega}{\partial X} - \frac{\partial \Psi}{\partial X}\frac{\partial \Omega}{\partial Y} = Pr\left(\frac{\partial^2 \Omega}{\partial X^2} + \frac{\partial^2 \Omega}{\partial Y^2}\right) + Ra\ Pr\frac{\partial \theta_f}{\partial X} \quad \text{.....(20)}$$

$$\frac{\partial \theta_f}{\partial \tau} + \frac{\partial \Psi}{\partial Y}\frac{\partial \theta_f}{\partial X} - \frac{\partial \Psi}{\partial X}\frac{\partial \theta_f}{\partial Y} = \frac{\partial^2 \theta_f}{\partial X^2} + \frac{\partial^2 \theta_f}{\partial Y^2} \quad \text{.....(21)}$$

2.3 Dimensionless Initial And Boundary Conditions

The initial and boundary conditions (9) and (10) in the dimensionless form are given by :

Dimensionless initial conditions

$$\theta_f = \theta_s = U = V = \Omega = \Psi = 0 \quad at\tau = 0 \quad \text{.....(22)}$$

Dimensionless boundary conditions $for\tau > 0$:

$$\theta = 1 \ , \ U = V = \Psi = 0 \quad atX = 0 \ , \ 0 < Y < \frac{H}{L} \quad \text{.....(23a)}$$

$$\theta = 0 \ , \ U = V = \Psi = 0 \quad atX = 1 \ , \ 0 < Y < \frac{H}{L} \quad \text{.....(23b)}$$

$$\frac{\partial \theta}{\partial Y} = 0 \ , \ U = V = \Psi = 0 \ , \Omega = -\frac{\partial^2 \Psi}{\partial Y^2} atY = 0 \ , 0 < X < 1 \quad \text{.....(23c)}$$

$$\frac{\partial \theta}{\partial Y} = 0 \ , \ U = V = \Psi = 0 \ , \Omega = -\frac{\partial^2 \Psi}{\partial Y^2} atY = \frac{H}{L} \ , 0 < X < 1 \quad \text{.....(23d)}$$

$$\theta_f = \theta_s \ , \ \frac{\partial \theta_f}{\partial X} = Kr\frac{\partial \theta_s}{\partial X} \ , U = V = \Psi = 0 \ , \Omega = -\frac{\partial^2 \Psi}{\partial X^2} atX = \frac{L_1}{L} andX = \frac{L_1+L_2}{L}, 0 < Y < \frac{H}{L} \quad \text{..(23e)}$$

where $\mathrm{Kr} = \frac{\mathrm{K_s}}{\mathrm{K_f}}$ is the thermal conductivity ratio.

The physical quantities of interest in this problem are the local and average Nusselt numbers, defined respectively by:

$$Nu = -\left(\frac{\partial \theta}{\partial X}\right)_{X=\frac{L1}{L},\frac{L1+L2}{L}} \quad ; \quad \overline{Nu} = \frac{1}{(H/L)}\int_0^{H/L} Nudy \quad \text{.....(24)}$$

3. Solution Procedure

The governing dimensionless partial differential equations are discretized to a finite difference form, the entire domain is subdivided into a mesh system, size (n*m), ensuring that the boundaries lie on grid points.

The appropriate finite difference scheme representations of the partial differential terms in the governing equations are cast and used to replace each of the terms.

The algebraic equations obtained from finite difference for the stream function were solved by (Line Successive Relaxation) method, while those for vorticity and temperature were solved by (Alternating Direction Implicit (ADI) Method With Relaxation Parameter) in two time step of$(\Delta\tau/2)$ for each direction.

The solution of resulting equations was obtained using line-by-line method, which results a Tri-diagonal matrix (TDM) solved numerically using Tri-diagonal matrix algorithm (TDMA). The criterion for convergence is examined according to a realistic condition for each state variable at each node as:

ISSN 2347-1921

$$\frac{\left|\phi_{i,j}^{new} - \phi_{i,j}^{old}\right|}{\left|\phi_{i,j}^{old}\right|} \leq 10^{-5} \qquad \text{.....(25)}$$

Where the subscripts i andj refer to a grid node, Ø is a general dependent variable (θ , Ω or Ψ). A computer programs in (Matlab) were built to execute the numerical algorithms which are mentioned above.

4. Numerical validation

In order to validate the numerical model a comparison was made with the results obtained by Belazizia, A., Benissaad, S. and Abboudi, S. (2012) for conjugate natural convection in a square enclosure with finite vertical wall thickness as shown in Fig.2 and Table 1. A good agreement between the obtained and reported results can be observed.

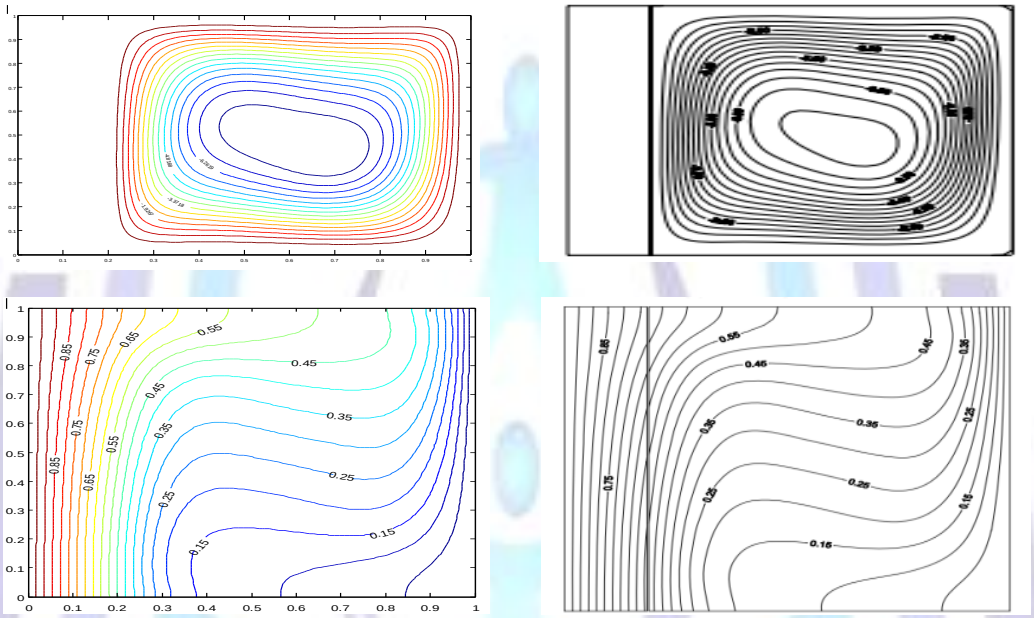

(a) (b)

Fig. 2 : Comparison of streamlines (top) and isotherms (bottom) at $Ra = 10^5, kr = 1, \frac{L1}{H} = 0.2$ (a) present study , (b) numerical results of BELAZIZIA (2012)

Table 1:The comparison between the obtained numerical results and the solution of BELAZIZIA

Ra	Kr	Results obtained by BELAZIZIA	Present Study $\overline{Nu}$
500	0.1 1	`0.382 1.03	0.383 1.01
10 000	0.1 1	0.41 1.57	0.41 1.55
100 000	0.1 1	0.461 2.35	0.460 2.31
1000 0000	0.1 1	0.516 3.40	0.571 3.39

ISSN 2347-1921

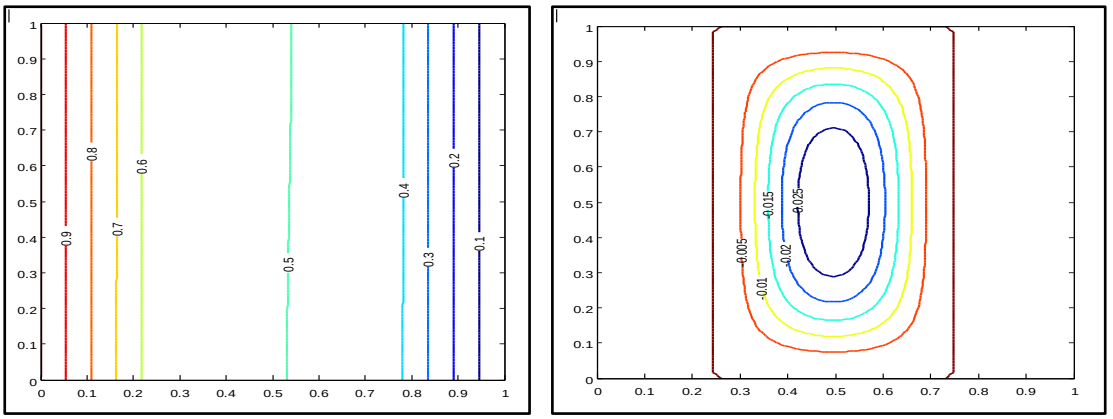

(a) L1/L2=0.5 , $\overline{Nu}$=0.1860, $|\Psi_{max}|$=0.0300

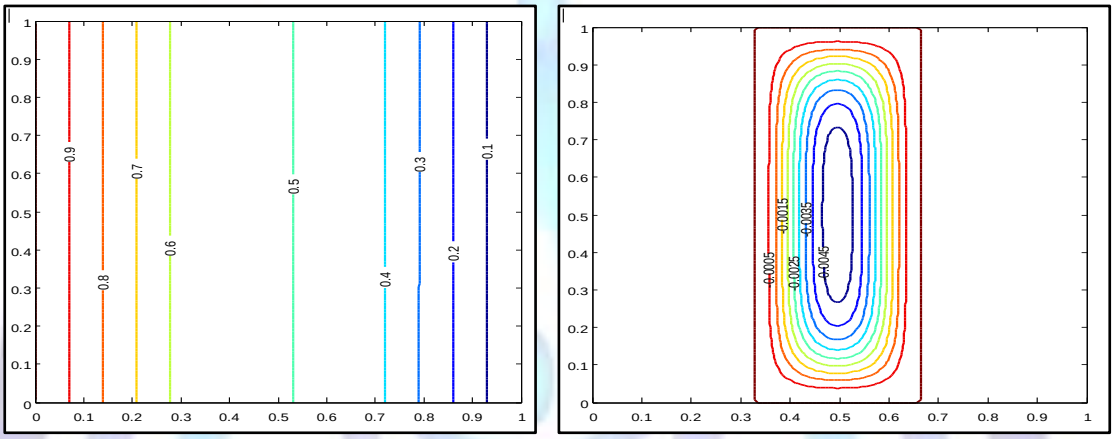

(b) L1/L2=1 , $\overline{Nu}$=0.1456, $|\Psi_{max}|$=0.0048

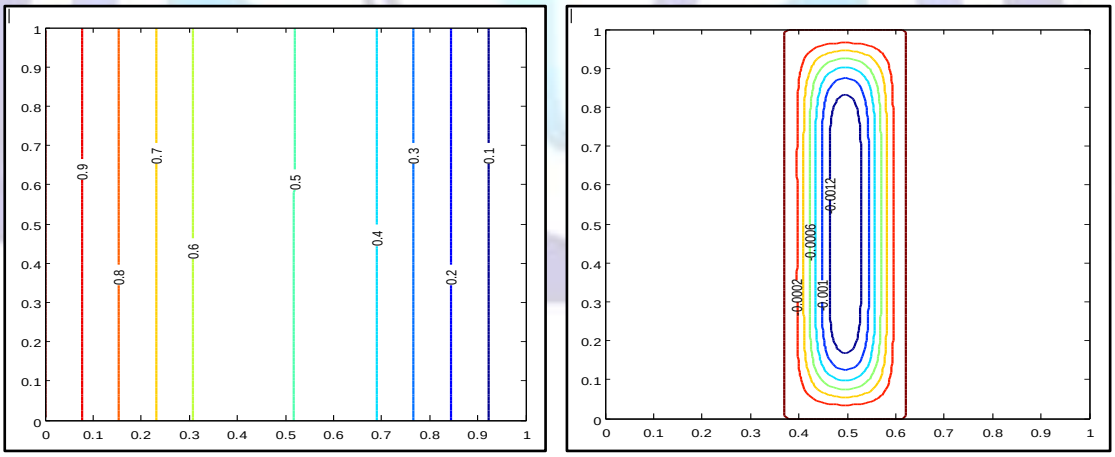

(c)L1/L2=1.5 , $\overline{Nu}$=0.1314, $|\Psi_{max}|$=0.0014

Fig. 3 : Isotherms (left) , Streamlines(right) at Ra=1000 , kr=0.1

ISSN 2347-1921

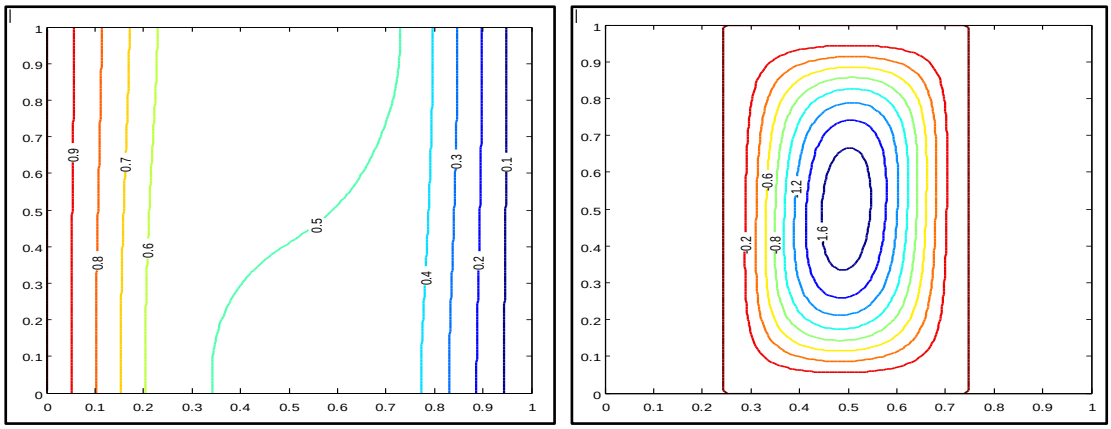

(a) L1/L2=0.5 , $\overline{Nu}$=0.1902, $|\Psi_{max}|$=1.7246

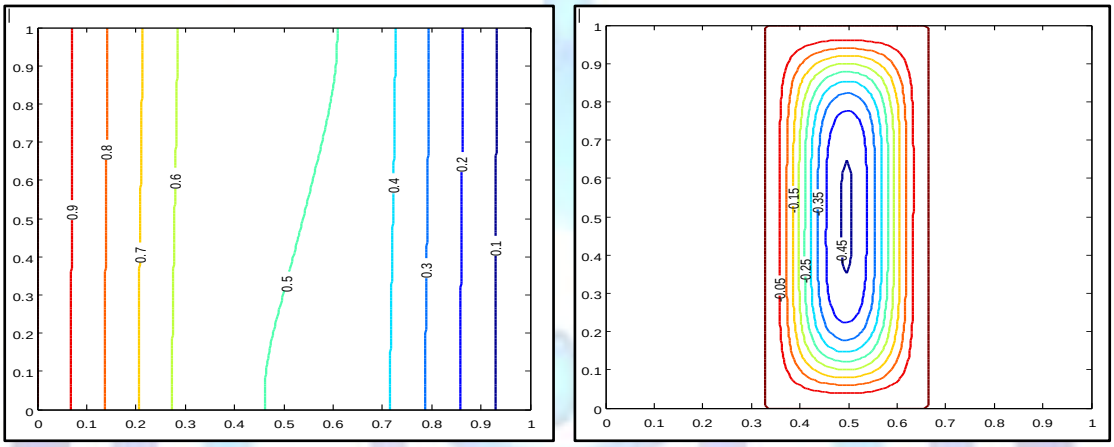

(b) L1/L2=1 , $\overline{Nu}$=0.1458, $|\Psi_{max}|$=0.4542

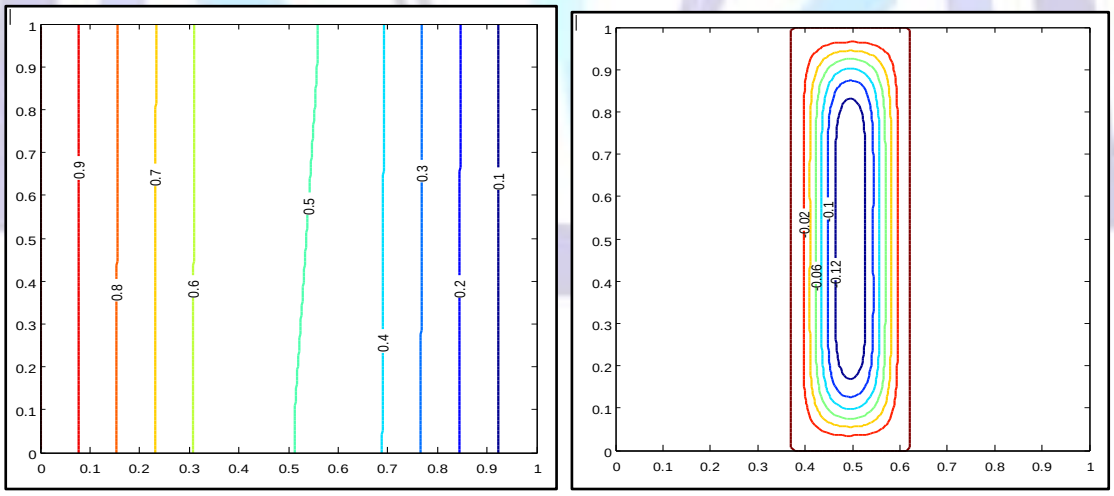

(c) L1/L2=1.5 , $\overline{Nu}$=0.1314, $|\Psi_{max}|$=0.1369

Fig. 4 : Isotherms (left) , Streamlines(right) at Ra=100000 , kr=0.1

ISSN 2347-1921

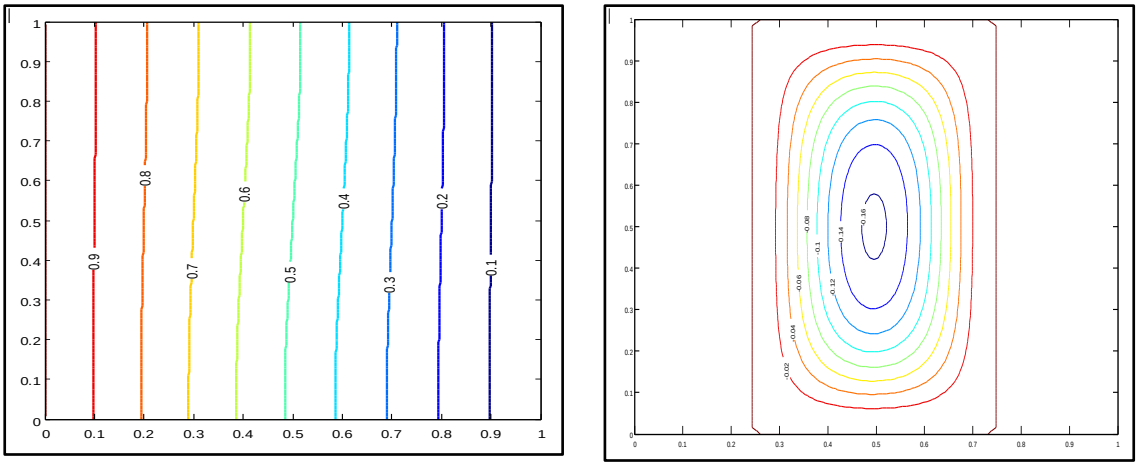

(a)L1/L2=0.5 , $\overline{Nu}$=1.0026, $|\Psi_{max}|$=0.1633

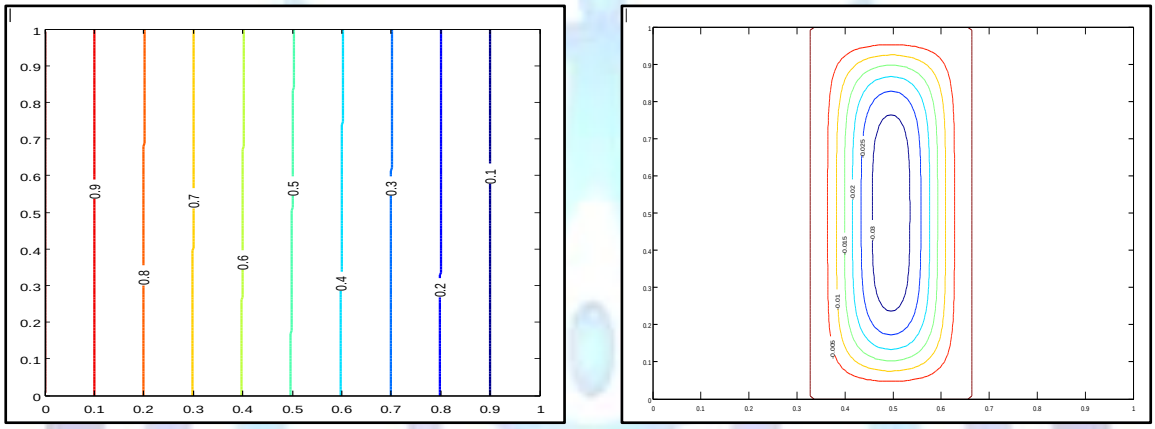

(b)L1/L2=1 , $\overline{Nu}$=1.0016, $|\Psi_{max}|$=0.0336

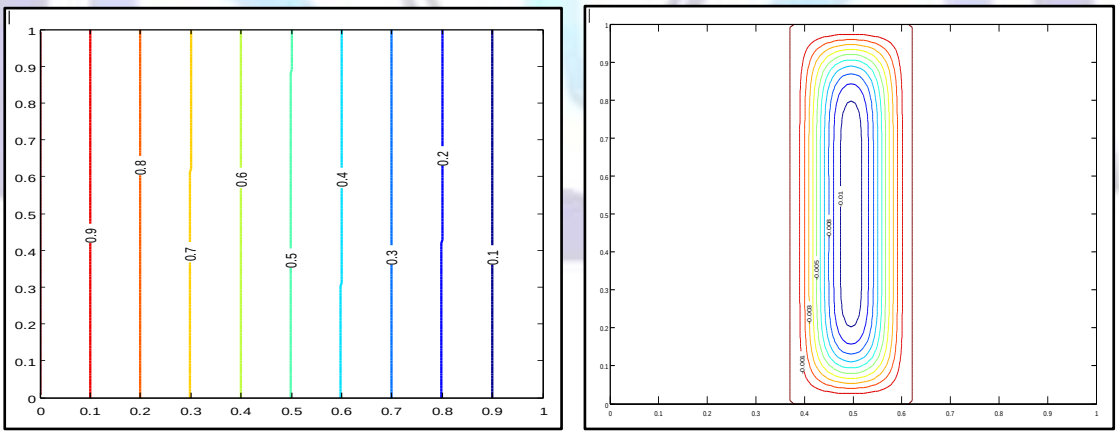

(c)L1/L2=1.5 , $\overline{Nu}$=1.0016, $|\Psi_{max}|$=0.0106

Fig. 5 : Isotherms (left) , Streamlines(right) at Ra=1000 , kr=1

ISSN 2347-1921

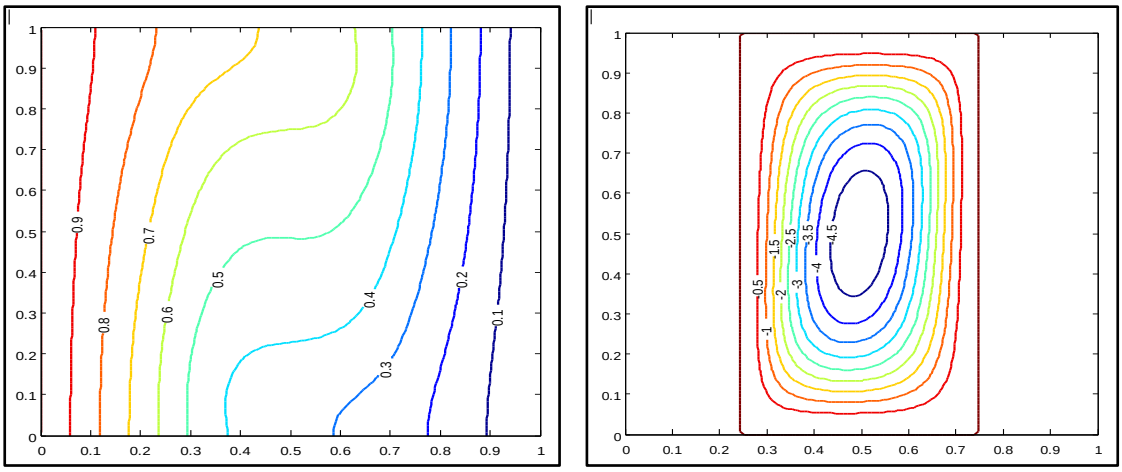

(a) L1/L2=0.5 , $\overline{Nu}$=1.3487, $|\Psi_{max}|$=4.8979

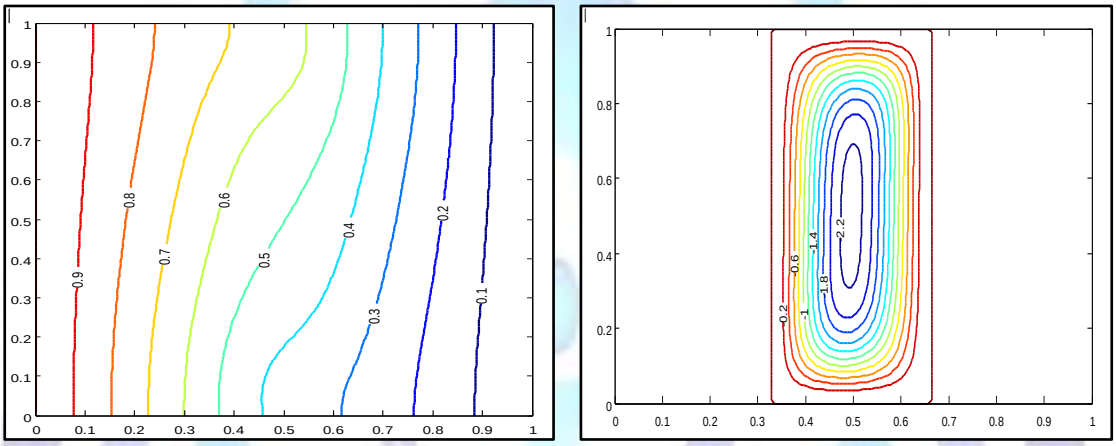

(b) L1/L2=1 , $\overline{Nu}$=1.0908, $|\Psi_{max}|$=2.2765

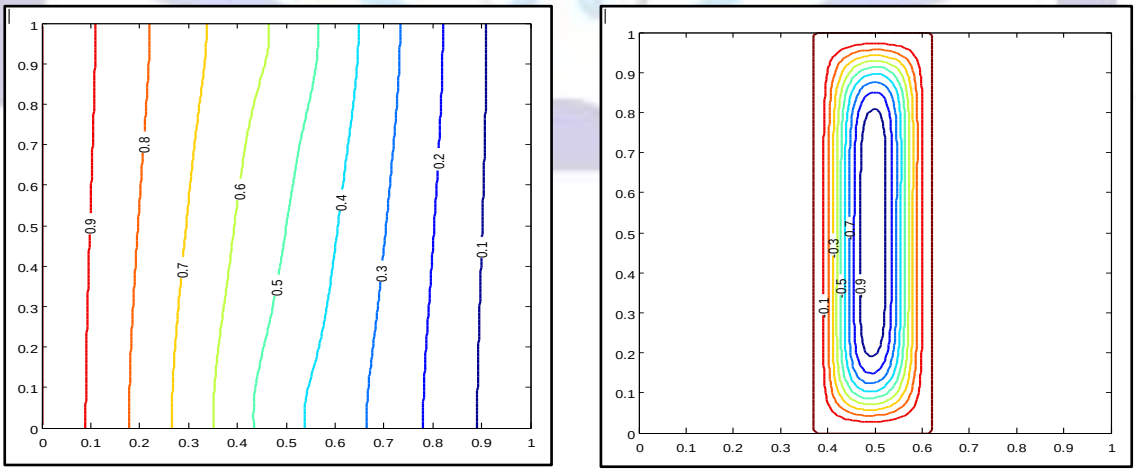

(c) L1/L2=1.5 , $\overline{Nu}$=1.0169 , $|\Psi_{max}|$=0.9849

Fig. 6 : Isotherms (left) , Streamlines(right) at Ra=100000 , kr=1

ISSN 2347-1921

5. Results and discussion

The results are generated for different values of the governing parameters, which are the Rayleigh number (1000<Ra<1000000), the Prandtl number (Pr=0.7), the wall to fluid thermal conductivity ratio (0.1≤Kr≤10), (left or right) solid to fluid thickness ratio ($0.5 \leq L_1/L_2 \leq 1.5$), the ratio of height of the model to its length $(H/L = 0.5,1,1.5)$ and the ratio of (left or right) solid thickness to the height $\left(D = \frac{L_1}{H} = 0.5\,, 0.6667\,, 0.75\right)$.

5.1 Effect of ratio of the (left or right) solid to fluid thickness

To show the effect of solid to fluid thickness ratio (L_1/L_2) on the thermal field and the circulation of the fluid in the enclosure, the isotherms and streamlines are presented in Figs. (3), (4), (5) and (6) for (Ra=1000,100000 , kr=0.1,1 , H/L=1).As (L_1/L_2) increases, the average Nusselt number decreases, which indicates conduction domination heat transfer in the system. It can see also from streamlines, that the strength of the fluid circulation is increasing with the increase of (L_1/L_2) and leads to reduce the maximum values of the dimensionless stream function $|\Psi_{max}|$.

5.2 Effect of Rayleigh number (Ra) and thermal conductivity ratio (kr)

For $(\frac{H}{L} = 1\,,\ \frac{L1}{L2} = 1\,, D = \frac{1}{3})$, Figs. (7) and (8), show the effect of both Rayleigh number (Ra) and thermal conductivity ratio (kr), on fluid motion in the enclosure. For different values of (kr) and increasing of the values of (Ra), we show the enhancement in the heat transfer by natural convection and leads to increase the average Nusselt numbers, and the same property for different values of (Ra), the increase of (kr) also tend to increase of the average Nusselt numbers, this is due to the thermal field in the fluid part, where the temperature gradient in the horizontal direction is increasing with the increase in (kr) (i.e. good conductive wall). A comparison is made for three cases of thermal conductivity ratio (kr =0.1,1,10). For poor conductive wall (panel (a) kr=0.1) where the solid wall is insulation material, the average Nusselt number have law values compare with those in panel (b) and (c). This is a logical result since reducing the thermal conductivity of the wall leads to the increase in thermal resistance of the overall system and therefore reducing the Nusselt number. Also the streamlines in Fig. (8), shows the relationship between thermal conductivity ratio (kr), Rayleigh number (Ra), and the maximum values of the dimensionless stream function $|\Psi_{max}|$. In both cases, the increase of (kr) for different values of (Ra) tend to increase of $|\Psi_{max}|$, and the same conclusion for increase in (Ra) for different values of (kr). The circulation pattern is in clockwise direction, with flow upward at the hot left interface and downward at the less hot right interface. For all values of (Ra) and kr the flow is symmetric, whereas for (kr=10) and $(Ra \geq 10^5)$ where the interface temperature is not uniform, the flow is asymmetric.

5.3 Average and Local Nusselt number

Fig.(9), shows the effect of the ratio of (left or right) solid thickness to height $(D = \frac{L1}{H})$ on the rate of heat transfer across the enclosure for the two cases of (Ra=1000 , 100000) and (kr = 0.1 , 1), We note that for (Ra=1000) and (kr = 0.1 , 1) with increasing (D), the average Nusselt number is decreasing until (kr =1), the relationship becomes constant nearly, then when the values of (kr >1), the increasing of (D) tends to increase the values of average Nusselt number because the natural convection inside the fluid part is driven by the temperature difference between the left and right interfaces. This difference is lower for walls with poor thermal conductivity, it becomes more important with the increase of (kr), and lead to increase the average Nusselt number. When (Ra=100000) and for all values of (kr), we see the reverse relation between (D) and $(\overline{Nu})$,that is, the increase of (D) corresponds the decrease of $(\overline{Nu})$.

Fig.(10), represents the relationship between (kr) and $(\overline{Nu})$ at (Ra=1000) with difference values of (D) when the height to the length ratio (H/L=0.5). For cases of$(D = \frac{1}{2}, \frac{2}{3})$, the increase of (kr) results increase of $(\overline{Nu})$ except when $(D = \frac{3}{4})$ for(kr ≤1), the relationship between(kr) and $(\overline{Nu})$ remains as in previous cases,but when (kr >1), we note the change in relationship, (i.e. kr increasing→$\overline{Nu}$ decreasing).

ISSN 2347-1921

The variation of the local Nusselt number along the solid-fluid and fluid-solid layer interfaces $(X = \frac{L1}{L}$ and $X = \frac{L1+L2}{L})$ are shown in Fig. (11) for constant (Ra=1000) and$(D = 0.5)$. For the law values of (kr), the local Nusselt number have law values comparing with those at high values of (kr), and the difference among values of Local Nusselt numbers for $(kr \geq 1)$ is greater than for $(kr < 1)$ as shown in Fig.(11).

5.4 Interface temperature

The variation of temperatures of left solid-fluid and right fluid-solid layer interfaces $(X = \frac{L1}{L}$ and $X = \frac{L1+L2}{L})$ are shown in Fig. (12) for different values of the ratio of (left or right) solid thickness to the height $(D = 0.5,0.6667,0.75)$ at constant (kr =1) and (Ra=1000). It is observed that the temperature gradients with respect of Y-direction are decreasing with increasing of the values of (D) in both interfaces $(X = \frac{L1}{L})$ and $(X = \frac{(L1+L2)}{L})$. There is a direct relation between $(D = \frac{L1}{H})$ and the solid to fluid thickness ratio $(\frac{L1}{L2})$ (i.e. $(\frac{L1}{L2})$ increases with increasing of (D) and vice versa), hence the increasing of (D) results to reduce the temperature difference between the two interfaces and therefore reducing the average Nusselt number.

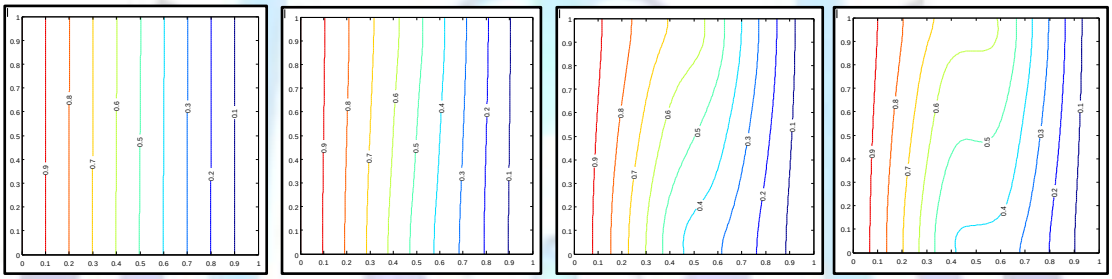

(1):Kr=0.1(a) $\overline{Nu} = 0.1456$ (b)$\overline{Nu} = 0.1456$(c) $\overline{Nu} = 0.1458$ (d) $\overline{Nu} = 0.148$

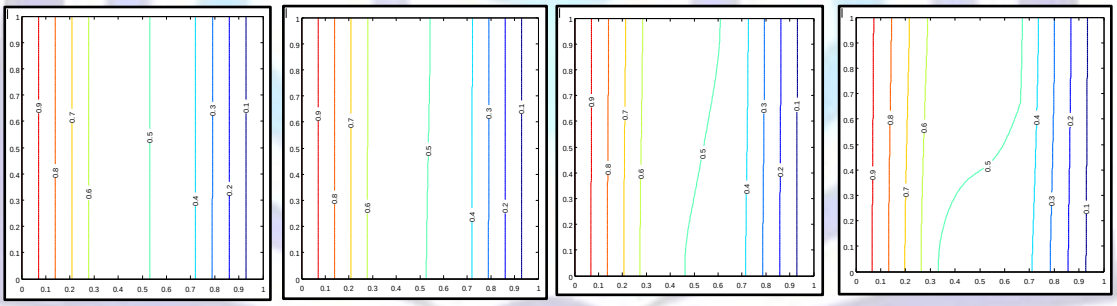

(2):Kr=1(a) $\overline{Nu} = 1.0016$ (b) $\overline{Nu} = 1.0042$ (c) $\overline{Nu} = 1.0908$ (d) $\overline{Nu} = 1.2479$

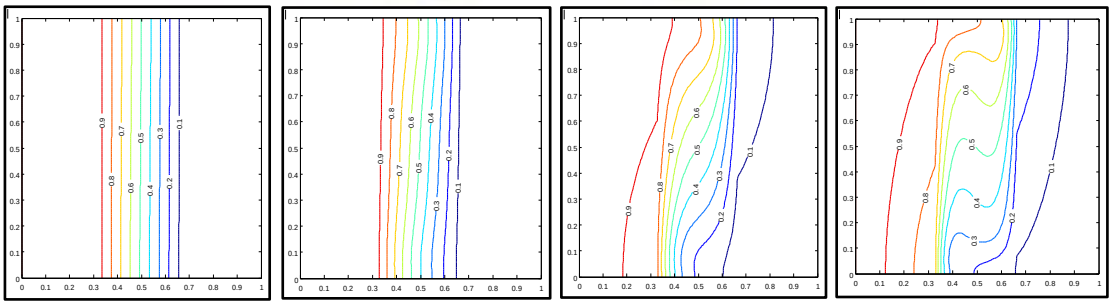

(3):Kr=10(a) $\overline{Nu} = 2.4852$ (b) $\overline{Nu} = 2.5322$(c) $\overline{Nu} = 3.6398$ (d) $\overline{Nu} = 5.6708$

Fig. 7 : isotherms for H=L , L1/L2=1, L1/ H =0.333 ,Kr=0.1,1,10 : (a) Ra=1000,(b) Ra=10000, (c) Ra=100000 and (d) Ra=1000000

ISSN 2347-1921

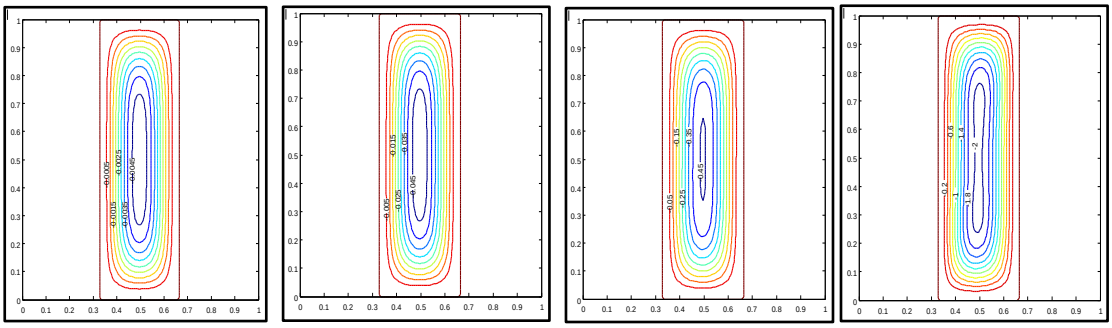

(1):Kr=0.1 (a) $|\Psi_{max}|$=0.0048 (b) $|\Psi_{max}|$=0.0481 (c) $|\Psi_{max}|$= 0.4542 (d) $|\Psi_{max}|$=2.0670

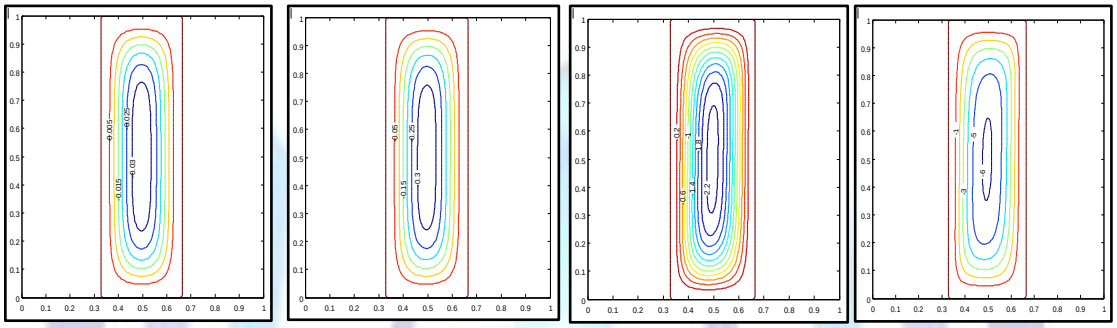

(2):Kr=1(a) $|\Psi_{max}|$=0.0336 (b) $|\Psi_{max}|$=0.3325 (c) $|\Psi_{max}|$= 2.2765 (d) $|\Psi_{max}|$= 6.1181

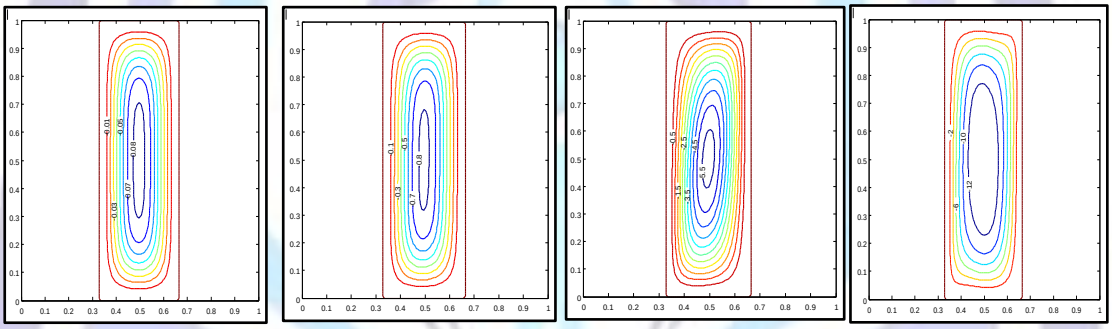

(3):Kr=10(a) $|\Psi_{max}|$=0.0834 (b) $|\Psi_{max}|$=0.8253 (c) $|\Psi_{max}|$=5.6994 (d) $|\Psi_{max}|$=13.9477

Fig. 8: streamlines for H=L , L1/L2=1, L1/ H =0.333 ,Kr=0.1,1,10 : (a) Ra=1000,(b) Ra=10000, (c) Ra=100000 and (d) Ra=1000000

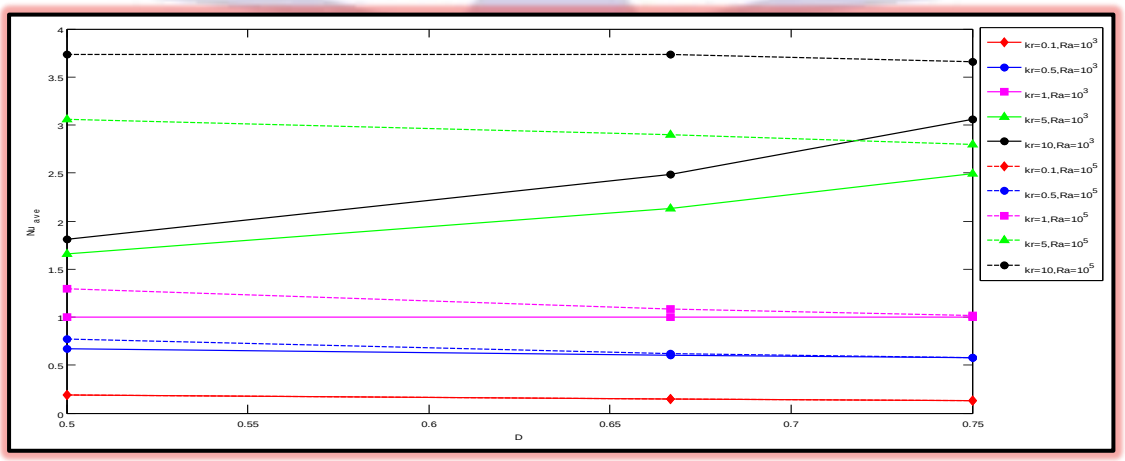

Fig. 9: Variation of $\overline{\mathrm{Nu}}$ with D

ISSN 2347-1921

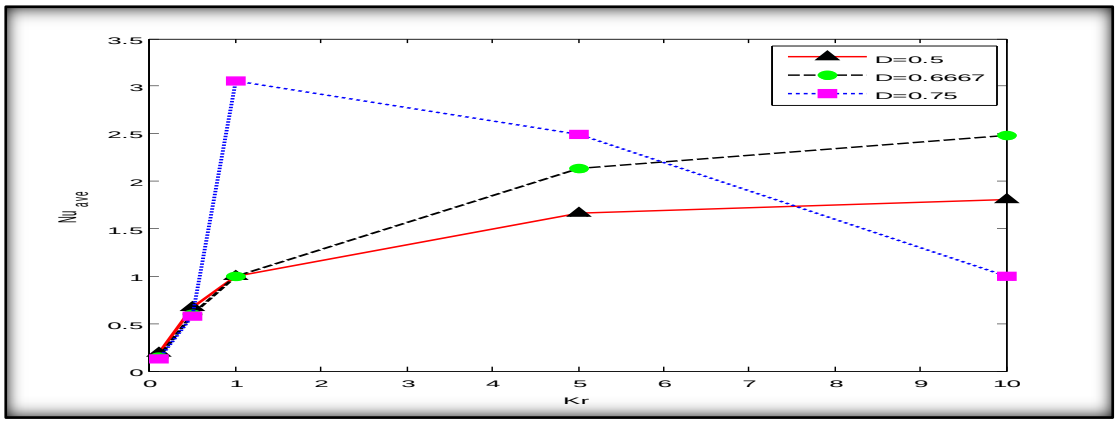

Fig.10: Variation of $\overline{Nu}$ with Kr at Ra = 1000 for difference value of D

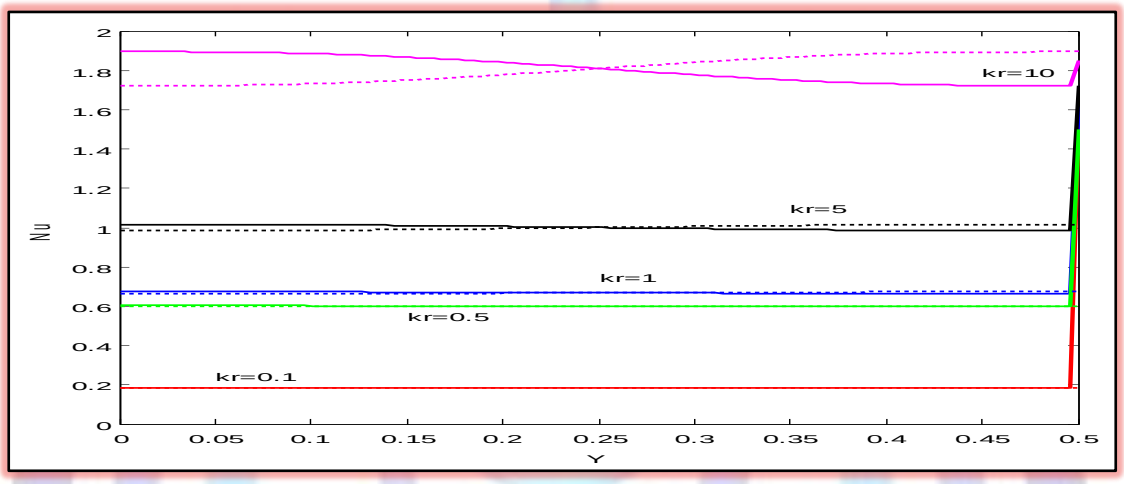

Fig. 11: Local Nusselt number of (solid-fluid)(—) and (fluid–solid)(…) layer interfaces at: Ra = 1000 and D = 0.5

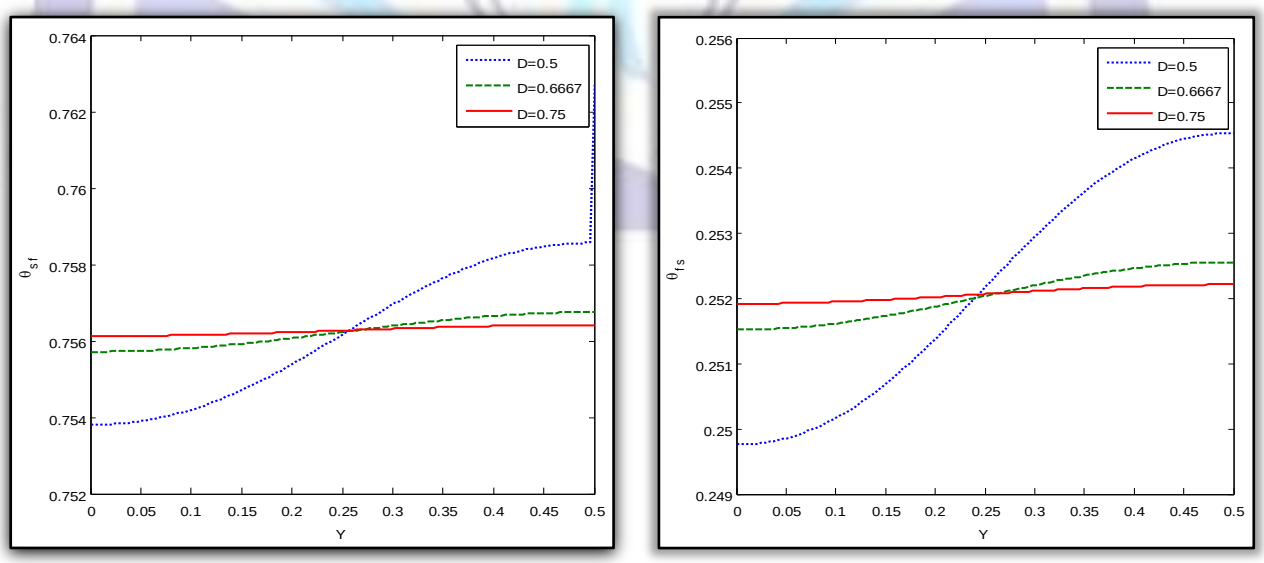

Fig. 12 : Variation of(left solid–fluid\right fluid-solid) interface temperature at constant kr = 1 and Ra = 1000

ISSN 2347-1921

6. Conclusion

A numerical study was employed to analyze the flow and heat transfer of air filled rectangular enclosure sandwiched between two equal- thickness walls. The vertical boundaries are isothermal at different temperatures whereas the horizontal boundaries are adiabatic. The governing parameters are the Rayleigh number (Ra), the Prandtl number (Pr), the solid to fluid thermal conductivity ratio (kr), solid to fluid thickness ratio (L_1/L_2) and the ratio of (left or right) solid thickness to the height ($D = \frac{L1}{H}$). The numerical results indicated that the effect of solid to fluid thickness ratio (L_1/L_2)on the thermal field and the circulation of the fluid in the enclosure such that if (L_1/L_2) increases, the average Nusselt number decreases, which indicates conduction domination heat transfer in the system. It can see also from streamlines, that the strength of the fluid circulation is increasing with the increase of (L_1/L_2) and leads to reduce the maximum values of the dimensionless stream function $|\Psi_{max}|$. For different values of (kr), the increase of (Ra)lead to enhancement in the heat transfer by natural convection and increase the average Nusselt numbers, also we get the same property by increasing (kr)for different values of (Ra). At interfaces when (Ra=1000) and the ratio of (left or right) solid thickness to the height (D =0.5), for law values of (kr) (poor conductive wall),the Local Nusselt numbers have law values comparing with those at high values of (kr). For (kr =1) and (Ra=1000), the temperature gradients with respect of Y-direction are decreasing with increasing of the values of (D) in both interfaces $(X = \frac{L1}{L})$ and $(X = \frac{(L1+L2)}{L})$ and therefore reducing the average Nusselt numbers.

REFERENCES

[1] Abdelbaki, A. andZrikem, Z., Simulation numérique des transfersthermiquescouplés à travers les paroisalvéolairesdesbâtiments // Int. J. Therm. Sci. (1999). Vol.38, P. 719-730.

[2] Aminossadati, S.M. and Ghasemi, B., Natural convection cooling of a localized heat source at the bottom of a nanofluid-filled enclosure, European Journal of Mechanic B/Fluids, 28 (2009), pp. 630–640.

[3] Basak, T., Roy, S., and Pop, I., Heat flow analysis for natural convection within trapezoidal enclosures based on heatline concept, International Journal of Heat and Mass Transfer (2009), 52: 2471-2483.

[4] Baytas, A.C., Liaqat, A., Grosan, T., and Pop, I., Conjugate natural convection in a square porous cavity, Heat Mass Transf. 37, (2001), pp. 467–473.

[5] Belazizia, A., Benissaad, S., and Abboudi, S., Effect of wall conductivity on conjugate natural convection in a square enclosure with finite vertical wall thickness, Adv. Theor. Appl. Mech., Vol. 5, (2012), no. 4, 179 – 190.

[6] Dalal, A. and Das, M.K. (2008), Heatline method for the visualization of natural convection in a complicated cavity, International Journal of Heat and Mass Transfer 51: 263-272.

[7] Holman, J.P. (1990), Heat transfer, New York: McGraw-Hill Press.

[8] Jones, I.P., A numerical study of natural convection in an air-filled cavity: comparison with experiment, Numer. Heat Transfer 2(1979), 193-213.

[9] Kikuchi, Y. (2004), Natural convection of liquid metal in square cavity.Proc.37th National Heat Transfer Symposium of Japan, 1, pp.343-344.

[10] Kim, D.M. and Viskanta,R. (1984), Study of effects of wall conductance on natural convection in differently oriented square cavities, Journal of Fluid Mechanics 144: 153-176,

[11] Kimura, S., Kiwata, T., Okajima, A., and Pop, I.,Conjugate natural convection in porous media, Adv. Water Resour. 20 (1997),111–126.

[12] Saeid, N.H. (2007), Conjugate natural convection in a porous enclosure: effect of conduction in one of the vertical walls, International Journal of Thermal Sciences 46: 531-539.

[13] Varol, Y., Oztop, H.F., andKoka, A., Entropy generation due to conjugate natural convection in enclosures bounded by vertical solid walls with different thicknesses, Int. Comm. Heat Mass Transf. 35, (2008), pp.648–656.

[14] Yedder, R.B. and Bilgen, E. (1997), Laminar natural convection in inclined enclosures bounded by a solid wall, Heat and Mass Transfer 32: 455-462.